Hybrid Technique for Vibration Control using Synchronized Switch Damping on Inductor Modal Approach and Shape Memory Alloy Integration

Hadja Yakoubi[1*], Aida Cherif[2], Mounir Meddad[3]

[1]*Laboratoire Matériaux et Systèmes Electroniques, Laboratoire Matériaux intelligents et énergies renouvelables, Mohammed El Bachir EIIbrahimi University, Bordj Bou Arreridj, Algeria; E-mail: hadja.yakoubi@univ-bba.dz*

[2,3] *Laboratoire Matériaux intelligents et énergies renouvelables, Mohammed El Bachir EIIbrahimi University, Bordj Bou Arreridj, Algeria.*

Abstracts: Vibration control is a critical aspect of various engineering applications, including automotive and aerospace systems. This research paper presents a novel approach to enhance the performance of the Synchronized Switch Damping on Inductor (SSDI) technique by incorporating Shape Memory Alloys (SMAs). SSDI has proven effective in managing energy dissipation during electronic switching transitions, mitigating voltage spikes and reducing electromagnetic interference. However, the method consumes a substantial amount of energy. In this study, we propose a hybrid approach that combines the benefits of SSDI with the unique properties of SMAs to achieve improved vibration control. The integration of SMAs introduces a semi-passive element to the system, exploiting the inherent properties of these alloys to undergo reversible shape changes in response to external stimuli. By strategically placing SMAs within the vibration-prone components of the system, we aim to harness the mechanical forces generated during shape recovery to counteract and dampen vibrations. This innovative approach aims to capitalize on the efficient energy conversion capabilities of SMAs, thus minimizing the additional energy consumption associated with traditional semi-passive methods. The research involves theoretical modeling and simulation studies to assess the effectiveness of the proposed technique. Preliminary results demonstrate a significant reduction in vibration amplitudes and enhanced damping capabilities, validating the potential of the integrated SSDI-SMA system. The findings of this study not only contribute to advancements in vibration control methodologies but also provide insights into the broader applications of SMA-enhanced semi-passive techniques in improving the overall performance and efficiency of systems.

Keywords: Vibration Control, Shape Memory Alloys, SSDI Modal, Smart Materials.

1. INTRODUCTION

All mechanical systems are subjected to different conditions that can lead to the appearance of vibratory movements. Vibration is a major scientific and technological challenge in many industrial applications and fields, such as instrumentation, automotive, aviation and space, where vibration can be an annoying source and can disrupt the system's operation. Vibration reduction may be accomplished in a variety of ways, depending on the situation; the most frequent being stiffening, damping, and isolation [1]. Damping systems that use a piezoelectric material as an electromechanical device have received a lot of attention. These materials are ideal for creating smart materials or buildings. They are bonded to or integrated into the structure as sensors, actuators, or both as bulk patches, piezo-fiber composites (PFC), or thick or thin layers. [2]. Piezoelectric materials consist of acting on the mechanical state of the structures by modulating the electric field applied to the material to control the vibrations by introducing strong non-linear values to the voltage generated by the piezoelectric elements for manipulation [3].

Among these vibration-damping techniques are synchronized switch damping (SSD) techniques originally developed by Richard and Guyomar [4] and [5]. The work of this article is related to the study of a particular technique for handling this voltage, where this technique increases the electromechanical conversion effect of piezoelectric materials based on the SSD technique, called SSDI technology. It is characterized by its self-actuation using converted electrical energy. It consists of reversing the voltage when it reaches its maximum, which is controlled by an electronic switch but cannot control vibration modes due to the number of low-amplitude voltage signals that must be reversed in a short and insufficient time to maximize transducer voltage, we therefore suggest SSDI modal technology. The principle of how to generate and improve the voltage of a piezoelectric element close

to the target standard speed stage by using some of the non-target potential energy [6].

Shape memory alloy (SMA) is also an attractive smart material that could be used as a stiffness-tuning element in an adaptive tuned vibration absorber (ATVA) [7]. Shape memory alloys (SMAs) are a class of metallic materials that exhibit a unique shape memory effect, which allows them to return to their original shape after being deformed when subjected to an appropriate thermomechanical loading process. This makes SMA a good field for studying non-linear systems using a mechanical and adaptive approach [8].

This research endeavors to contribute to the evolution of vibration control methodologies by introducing a novel approach that amalgamates the strengths of SSDI with the unique properties of Shape Memory Alloys (SMAs). When these systems are represented in intelligent vibration control materials, applications become adaptable and scalable. These systems consist of coupling piezoelectric materials with shape memory alloys. The research methodology encompasses theoretical modeling and simulation studies to comprehensively assess the proposed hybrid approach's effectiveness. Preliminary results from these studies demonstrate a significant reduction in vibration amplitudes and enhanced damping capabilities, providing early validation of the hybrid system's potential.

2. MODAL SSDI CONTROL

2.1. SSDI Control

The implementation of SSDI (Synchronized Switch Damping on Inductor) techniques consists of adding a switching device in parallel with the piezoelectric elements; this device is a simple electronic switch. The switch is in series with a coil of inductance LI [9]. The switch is usually open, except when a moving extremum is detected.

The piezoelectric element is switched intermittently from the open circuit to a specific electrical limit condition synchronously with the structural movement. The principles of the SSDS and SSDI techniques are based on the detection of maximum and minimum voltage values (switching points). Specifically, in the SSDI circuit, the switch is briefly closed when an extremum of displacement (or voltage) is detected. Consequently, the internal capacity of the piezoelectric element (C0) and the inductance (L1) constitute an oscillating circuit. The voltage of the piezoelectric element is reversed after half a period of the resonant circuit (Δtje) when the switch is again opened. The inversion time is proportional to the inductance.

$$t_{is} = \pi\sqrt{C_0 L_1} \quad (1)$$

The voltage inversion imperfection is due to losses in the inversion network, the reversed voltage V_{after} is lower than the voltage prior the inversion V_{prior}. An inversion factor γ is defined as :

$$V_{after} = -\gamma V_{prior} \quad (2)$$

This γ coefficient is related to the electrical quality factor of the (L, C_0) oscillating network [5]

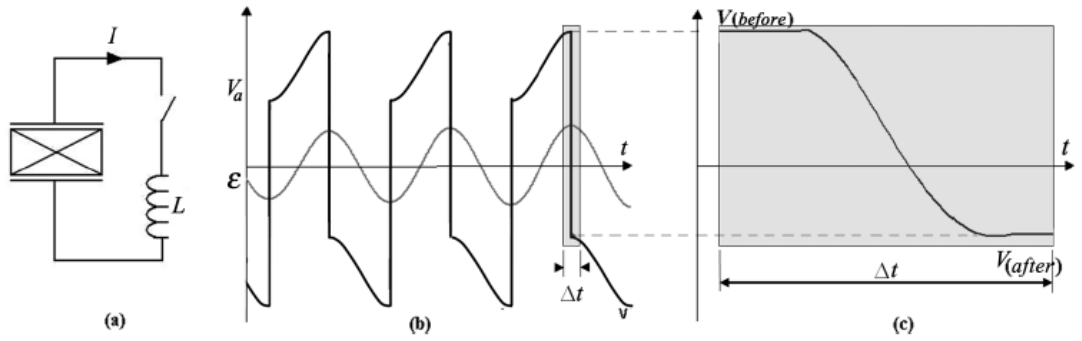

Figure 1. (a) The SSDI electrical circuit; (b) typical waveforms for a sinusoidal excitation, where V_a is the piezoelectric actuator voltage and ε is the voltage corresponding to the strain; (c) zoomed view of the voltage oscillation for inversion [5].

2.2. Modal SSDI Control

The modal SSDI control was developed because of the disability of the previous control in the case of broadband excitation. It is a hybridization technique of semi-active and active control. Figure 2 summarizes the SSDI-Modal strategy; its principle is synchronizing the switch sequence on a given modal coordinate instead of the voltage. The voltage inversion can be controlled by the extrema of the modal displacement. For obtaining the modal displacements q, which cannot be directly measured, it is necessary to use a modal observer as implemented by Harari and Chérif [10].

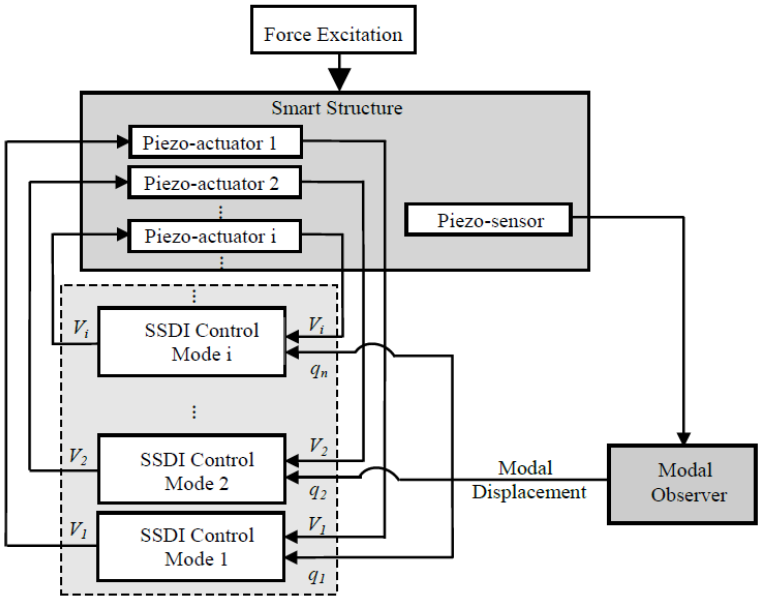

Figure 2. Principle of Modal-SSDI control [10].

3. Analytical modelling of the bilame effect

Bimetallic effects involve the deformation caused by differential heating in a layered structure comprising a material with a high coefficient of thermal expansion and another with a low coefficient of thermal expansion. The pioneering investigation into this phenomenon was carried out by S. Timoshenko, who examined the behavior of bimetal strips used in thermostats [11].

A bimetallic strip in the form of a beam, embedded on one side and flat at the initial state (Figure 3) takes the form of an arc of a circle when the temperature changes. The radius of curvature is given by the following expression [11]:

$$\frac{1}{R_T}-\frac{1}{R_0}=\frac{6(\alpha_2-\alpha_1)(1+m)^2}{3(1+m)^2+(1+mn)\left(m^2+\frac{1}{mn}\right)}.\frac{T-T_0}{s} \quad (3)$$

with :

R_T : radius of curvature at target temperature T, R_0- radius of curvature at reference temperature T_0, $m=\frac{S_1}{S_2}$: ratio of the thicknesses of the two layers , $n=\frac{Y_1}{Y_2}$: Young modules ratio of the two layers, α_1, α_2 : coefficients of thermal expansion (CTE). The index 2 corresponds to the high thermal expansion layer at the top of Figure 1.

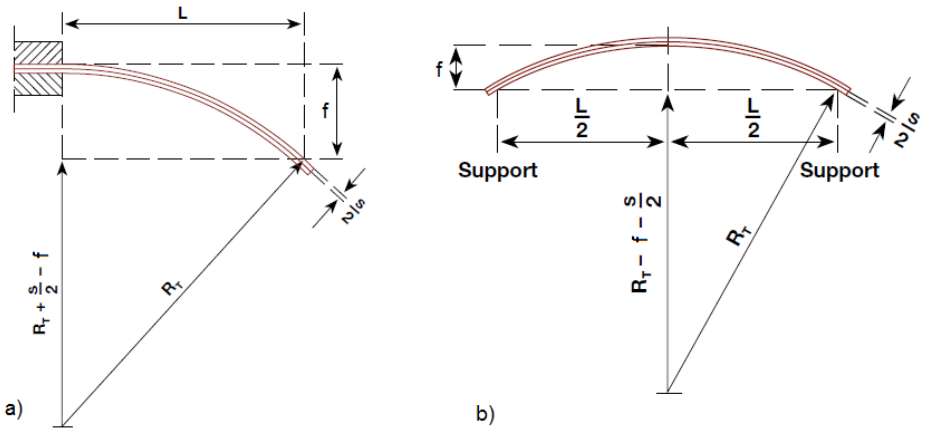

Figure 3. Deformation of a bimetallic strip in the form of a beam subjected to a temperature change: a) bimetallic strip embedded in one side.; b) bimetallic strip free.

If the bimetallic strip is flat at the reference temperature T_0, and that the thickness of the layers, as well as Young's modules are equal, equation (3) can be simplified to:

$$\frac{1}{R_T} = \frac{3(\alpha_2 - \alpha_1)}{2} \cdot \frac{T - T_0}{s} \qquad (4)$$

The radius of curvature of a bimetallic strip subject to a temperature variation is therefore inversely proportional to the difference in CTE, and the very variation. This means that a large difference in CTE or temperature implies a strong deformation. A thin bilame will deform more than a thick bilame. The specific curvature of the bilame is defined as :

$$k = \frac{3(\alpha_2 - \alpha_1)}{2} \qquad (5)$$

The arrow or maximum displacement over its length is calculated according to:

$$f = \frac{k}{2} \cdot \frac{(T - T_0)L^2}{s} \qquad (6)$$

This is a valid expression if the arrow is less than 10% of the length of the bimetallic strip. In case the displacement of the bimetallic strip is blocked at its tip, it develops an F force calculated according to:

$$F - F_0 = \frac{k}{2} \cdot \frac{Y(T - T_0)ls^2}{4L} \qquad (7)$$

With, F_0 : force at reference temperature T_0, usually equal to the ambient. The force is proportional to the width to length ratio : l/L and square of the thickness of the bimetallic strip. A thick bimetallic strip develops more strength due to the superior stiffness. Another case often encountered in practice is that of a free bilame, or simply supported (**Figure 3.b**). In this case, the arrow is calculated according to:

$$f = \frac{k}{2} \cdot \frac{(T - T_0)L^2}{4s} \qquad (8)$$

The resulting arrow is less than that of a beam embedded in a rib of the same length. This is due to the fact that the corresponding displacement is taken at the center, rather than at a free end.

If a force is applied to the centre of the bilame to limit its deformation, the arrow becomes:

$$f = \frac{k}{2} \cdot \frac{(T - T_0)L^2}{4s} - \frac{(F - F_0)L^3}{4ls^3Y} \qquad (9)$$

To cancel the arrow, must be applied a force equal to:

$$F - F_0 = \frac{k}{2}.\frac{Y(T - T_0)ls^2}{L} \qquad (10)$$

It is also the maximum force that the bimetal can develop during heating. It is four times higher for the free bimetal than for the bimetal embedded in one side. This is due to the higher stiffness that the free structure manifests.

A bimetal in the form of a beam that is constrained at its extremities is capable of flaring during heating. An initial form of sinus arc is considered, with the layer with a high coefficient of thermal expansion at the top and an arrow f0 down (Figure 2). During the heating of the high thermal expansion, the layer pulls the bimetal upwards and puts it into compression.

For a certain arrow f_1, an unstable position is reached. If the bimetal is heated more, it flares and changes the direction of its curvature. At this point, it will have an arrow f_2, pointing up. If we keep heating the structure, the arrow will continue to rise in the same direction.

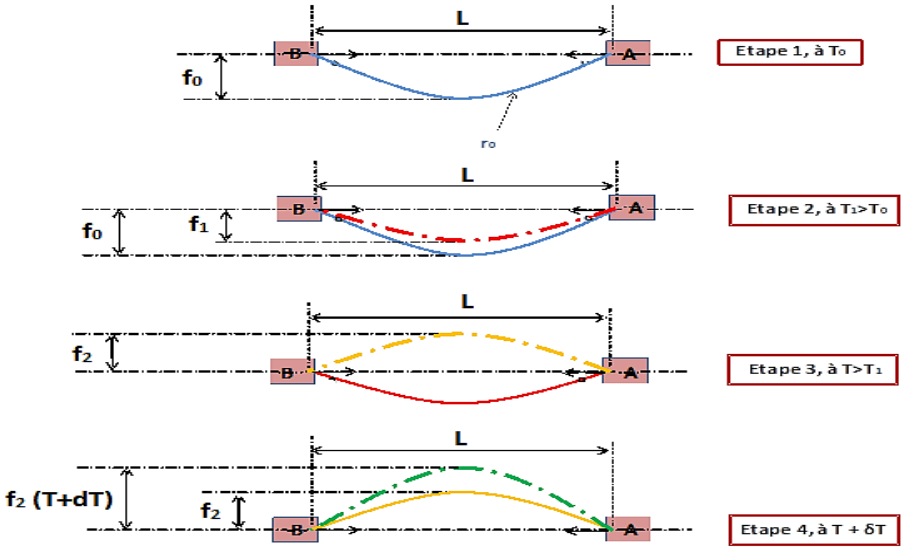

Figure 4. Deformation during heating of a bimetal at stationary ends.

4. Linearization of mathematical system model

Equation (7) initially models the force F as a linear function of temperature T, expressed as f(x) =A*x. To enhance accuracy, we are expanding this linear system into a non-linear one. This involves incorporating the depth-dependent effects of material expansion and deformation as a function of temperature. Figure 5 illustrates the calculation method for determining the expanded length based on the initial length L_0.

4.1. Demonstration

Figure (5) shows the demonstration of the non-linear system based on a linear system, which we used on our study to obtain the mathematical model.

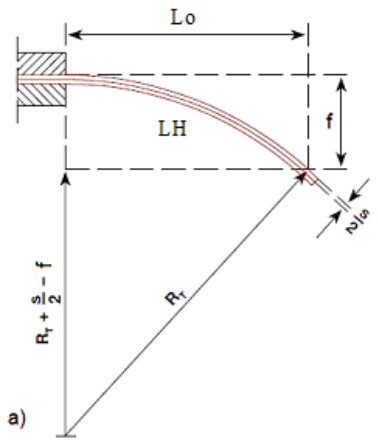

Figure 5. Inset bimetallic strip on one side.

From the figure 5 :

$$L_0 = \sin(\theta).R_T \qquad (11)$$

$$R_T = \frac{2s}{3(\alpha_2 - \alpha_1)(T - T_0)} \qquad (12)$$

$$L_{total} = L_H + dl_1 \qquad (13)$$

$$L_H = \arcsin(\theta).R_T \qquad (14)$$

$$L_{total} = \arcsin(\theta).R_T + dl_1 \qquad (15)$$

$$dl_1 = \alpha_1.L_0.\Delta T \qquad (16)$$

We take:

$$\Delta T = T - T_0 \qquad (17)$$

5. Smart-structure modeling

The proposed method here is a combination between the applications of innovative non-linear methods to the vibration damping control the semi-active control SSDI modal developed by Harari by the integration of the shape memory alloy with piezoelectric patches that give an additional mechanical force as a function of temperature.

The structure that will be used in the following simulations and analyses is a clamped steel plate equipped with four P188 piezoelectric inserts, as illustrated in Figure 6. Its dimensions and physical properties are given in Tables 1 and 2. This structure has been identified according to the previously described model. The measurement process and parameter identification are described in the study by Richard (2007). Table 2 presents the characteristics of PZT P189 piezoelectric inserts. Table 3 shows the characteristics of a form memory alloy (SMA):

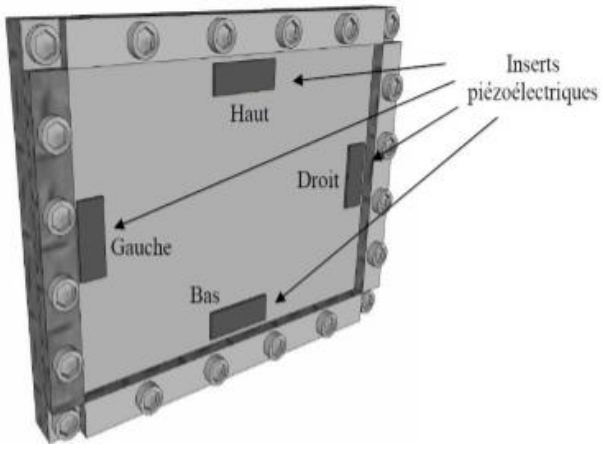

Figure 6. The plate is fixed on all four sides.

Table 1. Plate characteristic.

length	0.6 m
Width	0.4 m
Thickness	1 mm
Young modulus	210 GPa
Poisson ratio	0.345
Density	7500 Kg/m^3

Table 2: Characteristic of piezoelectric inserts P188.

Properties	**Symbol**	**Value**
Density	P	7650 Kg/m³
Short circuit complications	S_{11}^{E}	10.66.10^{-12} Pa^{-1}
	S_{12}^{E}	-3.34. 10^{-12} Pa^{-1}
	S_{13}^{E}	-4.52.10^{-12} Pa^{-1}
	S_{33}^{E}	13.25.10^{-12} pa^{-1}
Permittivity	ε_{33}^{T}	10.17 n F .m^{-1}
Piezoelectric coefficient	d_{13}	-108 p C .N^{-1}

Table 3: Shape Memory Alloy Characteristic (SMA).

Symbols	**Parameters**	**Values**
L0	Initial length	20×10^{-2}
Y	Young's modules	0.03×10^{9}
S	The thickness of the bimetal	2×10^{-4}
α_1 : alpha1	Thermal expansion coefficients (CTE).	2×10^{-4}
α_2 : alpha2	Thermal expansion coefficients (CTE).	170×10^{-4}
F0	The force at reference temperature T0	1×10^{-2}
L	Width	1×10^{-2}
K	Constant	
T	Temperatures	T= [0,300]

6. Results and Discussion

For the first step in our work we use the equation (7) to study changes in the mechanical force of the Shape-memory alloys as a function of temperature, by variation of the initial temperature T0 (T0=10°C, T0=20°C, T0=30°C) simulated using MATLAB software .

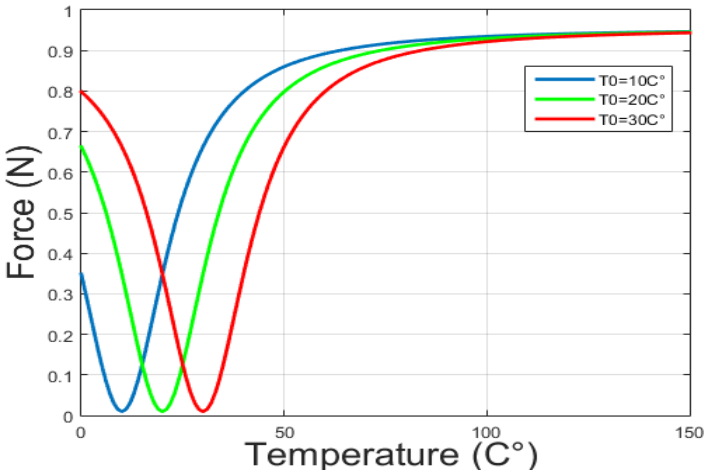

Figure 7. Expansion force of the Shape-memory alloys as a function of temperature at diffrent values of initial temperature (T0=10 C° , T0=20 C° T0=30 C°).

According to the three graphs :

Table 4. Values of maximum force F as a function of temperature.

T (°C)	T0=10	T0=20	T0=30
F (N) at T=50°C	0.8598	0.7981	0.6626
F (N) at T=100°C	0.9345	0.9293	0.9217
F (N) at T=150°C	0.9464	0.9451	0.9434

- The force of the alloy begins to increase until reaching its maximum value F≈ 0.94 N
- The three graphs of the force of the alloy start to stabilize at T=100°C.
- Reverse fit between the initial temperature T0 and the force of the alloy expansion.

6.1 Method of SSDI modal + SMA

This section is a simulation of the vibration control of the structure's single mode by applying the method non-linear methods to the vibration damping control SSDI madal control + the mechanical force of the shape memory alloys. We will conduct these studies using Matlab software by introducing the properties of shape memory alloys and its force expansion equation and using the Simulink block.

The excitation: a sinusoidal excitation in this case, the excitation is composed of the sum of four sine signals whose frequencies are those of the four modes of the structure.

For the additional mechanical force of the shape memory alloy, we use also a signal composed of the sum of four sine signals whose frequencies are those of the signal of the excitation , and the apmplutide of these signals correspond of three temperature values 40°C, 50°C, 70°C at an initial temperature T0=20°C.

The displacement graphs: The following figures present the comparison between the SSDI modal technique and the SSDI modal + shape memory alloy controlling the vibration of the structure.

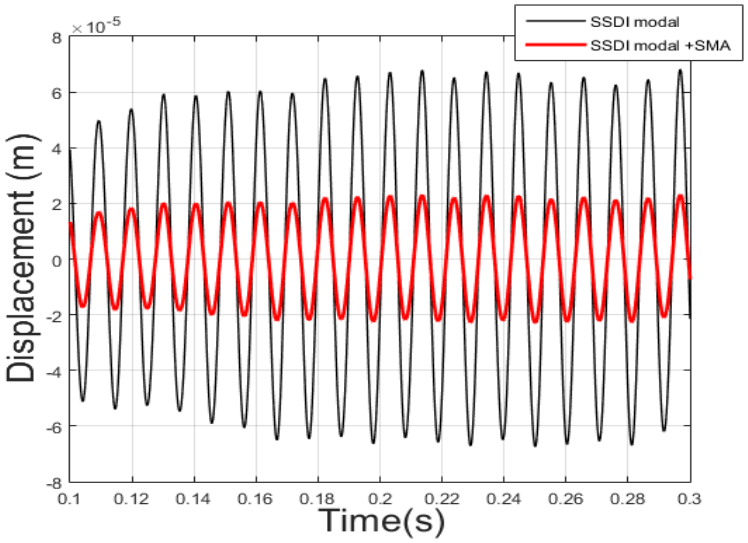

Figure 8. Displacement of the structure after SSDI modal control and SSDI modal + SMA control at T = 40°C as a function of time.

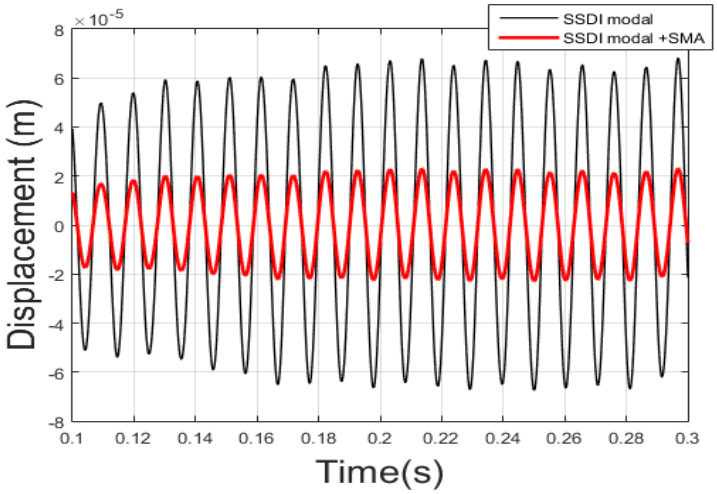

Figure 9. Displacement of the structure after SSDI modal control and SSDI modal + SMA control at T = 50°C as a function of time.

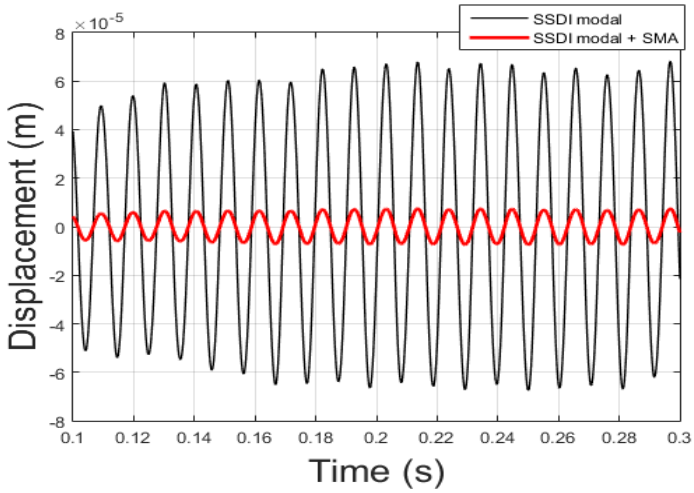

Figure 10. Displacement of the structure after SSDI modal control and SSDI modal + SMA control at T = 70°C as a function of time.

Table 5. Comparison of SSDI and SSDI+ SMA displacement values.

Temperature T(°C)	40	50	70
Displacement SSDI (u_{mean}) 1×10^{-5} m	3.7497	3.7497	3.7497
Displacement SSDI + SMA (u_{mean}) $\times10^{-5}$ m	1.2749	7.8744e-06	4.1247e-06
Percentage decrease	66%	79%	89%

Depending of the above graphs and the values of the table 5 we notice:

- A strong damping in the displacement amplitudes in SMA + SSDI control compared to SSDI.
- The higher value of the temperature, the better of displacement damping.

The system has two control effects:

- Modal SSDI method: this method absorbs a large amount of energy from the plate, which converts it into a high output voltage, as the damping is low.
- SSDI modal +SMA method: the shape memory alloy has a mechanical and subtractive effect, it gives a force against the movement of the plate to decrease the vibrations with the intervention of SSDI which absorbs the energy and dissipates it, so the damping is better but the voltage is decreased.

The second part of the validation methodology involves controlling the voltage variation of the actuator.

Voltage graphs :

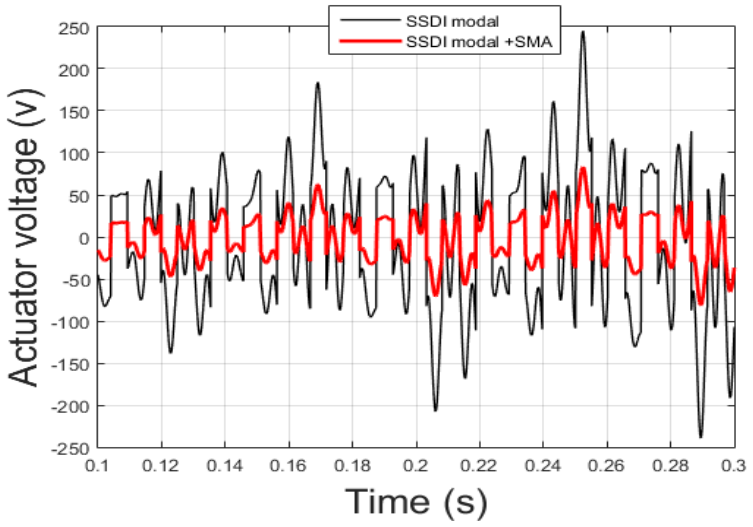

Figure 11. Actuator voltage in SSDI modal control and in SSDI modal + SMA control at T=40°C as a function of time.

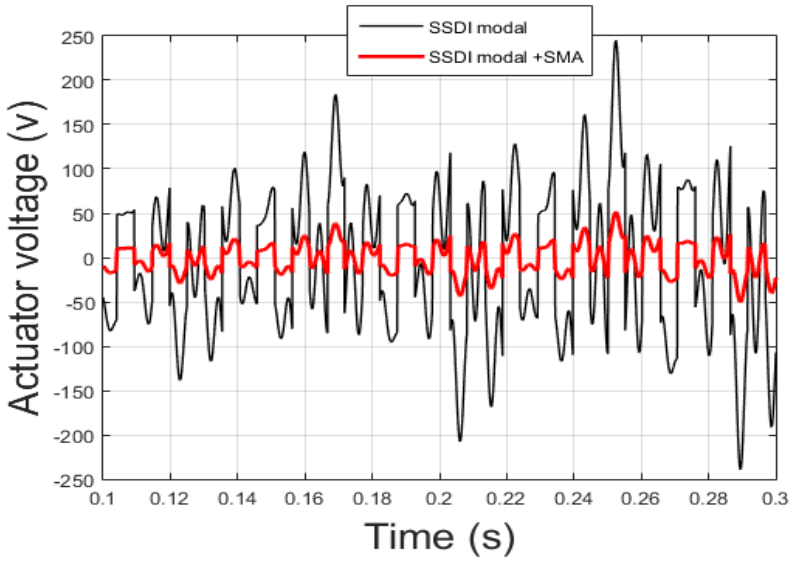

Figure 12 . Actuator voltage in SSDI modal control and in SSDI modal + SMA control at T=50°C as a function of time.

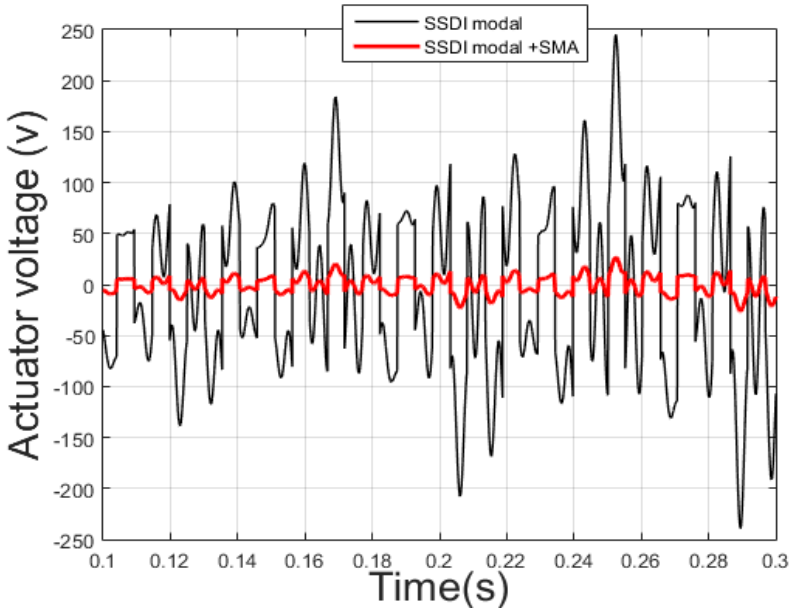

Figure 13. Actuator voltage in SSDI modal control and in SSDI modal + SMA control at T=70°C as a function of time.

Table 6. Comparison between SSDI modal and SSDI modal + SMA actuator voltage values.

T (°C)	40	50	70
The mean actuator voltage SSDI modal (v)	81.7864	81.7864	81.7864
The mean actuator voltage SSDI modal + SMA (v)	27.8074	17.1751	8.9965

Upon scrutinizing, the graphs illustrating actuator voltage values over time and referencing the data in Table 6, a discernible negative correlation emerges between temperature and actuator voltage. Notably, as the temperature rises, there is a corresponding decrease in the actuator voltage. This inverse relationship is attributed to the counteractive force generated by the shape memory alloy, which mitigates the movement of the structure, consequently leading to the reduction in actuator voltage.

CONCLUSIONS

In conclusion, this research has addressed a critical need for enhanced vibration control in engineering

applications, specifically within the realms of automotive and aerospace systems. The proven effectiveness of the Synchronized Switch Damping on Inductor (SSDI) technique in managing energy dissipation during electronic switching transitions laid the foundation for our innovative approach. By integrating Shape Memory Alloys (SMAs) into the system, we introduced a semi-passive element that undergoes reversible shape changes in response to external temperature.

The hybrid approach presented in this study strategically places SMAs within vibration-prone components, harnessing mechanical forces generated during shape recovery to counteract and dampen vibrations. Our findings from theoretical modeling and simulation studies demonstrate a significant reduction in vibration amplitudes and enhanced damping capabilities. These preliminary results validate the potential of the integrated SSDI-SMA system to revolutionize vibration control methodologies in engineering applications.

Moreover, the integration of SMAs introduces a novel dimension by minimizing the additional energy consumption traditionally associated with semi-passive methods. Leveraging the efficient energy conversion capabilities of SMAs addresses a longstanding concern in the field and paves the way for more sustainable and energy-efficient engineering solutions.

This research not only contributes to advancements in vibration control but also extends its implications to a broader spectrum of applications. The innovative combination of SSDI and SMAs opens avenues for improved overall performance and efficiency in various systems. As we conclude, we advocate for further exploration and implementation of SMA-enhanced semi-passive techniques, emphasizing their potential to reshape the landscape of engineering methodologies and contribute to a more sustainable future.

REFERENCES

[1] Kandasamy, R., Cui, F., Townsend, N., Foo, C. C., Guo, J., Shenoi, A., & Xiong, Y. (2016). A review of vibration control methods for marine offshore structures. Ocean Engineering, 127, 279-297.

[2] Richard, C., Harari, S., & Gaudiller, L. (2009, April). Enhanced piezoelectric voltage build-up for semi-active control of smart structures. In Active and Passive Smart Structures and Integrated Systems 2009 (Vol. 7288, pp. 709-720). SPIE.

[3] Chérif, A., Meddad, M., Belkhiat, S., Richard, C., Guyomar, D., Eddiai, A., & Hajjaji, A. (2014). Improvement of piezoelectric transformer performances using sshi and sshi-max methods. Optical and Quantum Electronics, 46, 117-131.

[4] Chérif, A., Richard, C., Guyomar, D., Meddad, M., Eddiai, A., Boughaleb, Y., ... & Sahraoui, B. (2015). Multimodal Vibration Damping of a Smart Beam Structure using Modal SSDI-Max.

[5] Chérif, A., Richard, C., Guyomar, D., Belkhiat, S., & Meddad, M. (2012). Simulation of multimodal vibration damping of a plate structure using a modal SSDI-Max technique. Journal of Intelligent Material Systems and Structures, 23(6), 675-689.

[6] Chérif, A., Richard, C., Guyomar, D., Belkhiat, S., & Meddad, M. (2012). Simulation of multimodal vibration damping of a plate structure using a modal SSDI-Max technique. Journal of Intelligent Material Systems and Structures, 23(6), 675-689.

[7] Kumbhar, S. B., Chavan, S. P., & Gawade, S. S. (2018). Adaptive tuned vibration absorber based on magnetorheological elastomer-shape memory alloy composite. Mechanical Systems and Signal Processing, 100, 208-223.

[8] Savi, M. A. (2015). Nonlinear dynamics and chaos in shape memory alloy systems. International Journal of Non-Linear Mechanics, 70, 2-19.

[9] Meddad, M., Eddiai, A., Cherif, A., Guyomar, D., & Hajjaji, A. (2016). Enhancement of electrostrictive polymer power harvesting using new technique SSHI-Max. Optical and Quantum Electronics, 48, 1-10.

[10] Harari, S., Richard, C., & Gaudiller, L. (2009). New semi-active multi-modal vibration control using piezoceramic components. Journal of Intelligent Material Systems and Structures, 20(13), 1603-1613.

[11] Timoshenko, S. (1925). Analysis of bi-metal thermostats. Josa, 11(3), 233-255.

DOI: https://doi.org/10.15379/ijmst.v10i3.3373